



Null-field method with discrete sources to electromagnetic scattering from layered scatterers

Adrian Doicu, Thomas Wriedt*

Institut für Werkstofftechnik, Badgasteiner Str.3, 28359 Bremen, Germany

Received 23 November 2000; accepted 18 February 2001

Abstract

A novel formulation for improving the numerical stability of the null-field method for highly elongated and flattened layered scatterers is presented. The key step in this approach is to approximate the surface current densities by the lowest-order multipoles located in the complex plane. The accuracy of the proposed method is investigated from a numerical point of view. © 2001 Elsevier Science B.V. All rights reserved.

1. Introduction

Electromagnetic scattering from layered scatterers can be computed by several methods. One of these approaches is the null-field method using localized sources [1,2]. Peterson and Ström [2] have shown that the problem of calculating the total \mathbf{T} matrix for one scatterer with several layers is algebraically much simpler than that of calculating the total \mathbf{T} matrix for several homogeneous scatterers. In the case of a multilayered scatterer a recursion formula for the \mathbf{T} matrix is obtained. However, numerical difficulties with the conventional, single spherical coordinate-based null-field method appear for scattering problems involving highly elongated and flattened layered scatterers.

The purpose of the present paper is to develop a null-field formalism using discrete sources. As discrete sources we use the system of distributed lowest-order multipoles. In fact we extend our method for homogeneous scatterers [3] to layered scatterers. As it was shown in the homogeneous case we expect that the use of discrete sources will extend the domain of applicability of the null-field method.

2. Basic equations

We consider the generic case of a two-layered scatterer defined by the closed surfaces S_1 and S_2 , where S_1 encloses S_2 according to Fig. 1. The exterior of S_1 is denoted by D_s , the interior of S_2 by D_2 and the domain between S_1 and S_2 by D_1 . The local origin O_i is attached to the closed surface S_i . The radius vector from the local

* Corresponding author.

E-mail address: thw@iwt.uni-bremen.de (T. Wriedt).

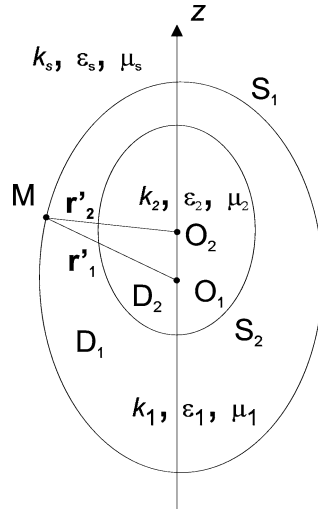


Fig. 1. Geometry of a composite scatterer consisting of two different homogeneous regions.

origin O_1 to a point M on the surface S_1 (or S_2) is denoted by \mathbf{r}'_1 and from the local origin O_2 to the point M by \mathbf{r}'_2 . The two layers are characterized by the relative constants $\epsilon_i, \mu_i, i = 1, 2$, and the corresponding wave numbers are $k_i = k\sqrt{\epsilon_i\mu_i}, i = 1, 2$, where $k = \omega/c$. The wave number for the free space is $k_s = k\sqrt{\epsilon_s\mu_s}$.

Let us rewrite the basic equations for the conventional null-field method in a slightly different form as given by Peterson and Ström [2]. Application of the equivalence principle reduces the two-layered scattering problem into three subproblems. For each subproblem, surface current densities are set up to create the actual field in the region of interest and a null field elsewhere. Let $\mathbf{e}_j, \mathbf{h}_j$ be the surface current densities acting on the closed surface S_j . For the subproblem corresponding to the domain D_s we consider the null-field condition inside an inscribed sphere of S_1 . This leads to the following set of integral equations for the surface current densities \mathbf{e}_1 and \mathbf{h}_1 :

$$\int_{S_1} \left[[\mathbf{e}_1^{\mathcal{N}}(\mathbf{r}'_1) - \mathbf{e}_0(\mathbf{r}'_1)] \cdot \begin{pmatrix} \mathbf{N}_{-mn}^3(k_s\mathbf{r}'_1) \\ \mathbf{M}_{-mn}^3(k_s\mathbf{r}'_1) \end{pmatrix} + j\sqrt{\frac{\mu_s}{\epsilon_s}} [\mathbf{h}_1^{\mathcal{N}}(\mathbf{r}'_1) - \mathbf{h}_0(\mathbf{r}'_1)] \cdot \begin{pmatrix} \mathbf{N}_{-mn}^3(k_s\mathbf{r}'_1) \\ \mathbf{M}_{-mn}^3(k_s\mathbf{r}'_1) \end{pmatrix} \right] dS(\mathbf{r}'_1) = 0. \tag{1}$$

For the subproblem corresponding to the domain D_1 we consider the null-field conditions outside a circumscribed sphere of S_1 and inside an inscribed sphere of S_2 . The resulting system of integral equations relates the surface current densities \mathbf{e}_1 and \mathbf{h}_1 to \mathbf{e}_2 and \mathbf{h}_2 , that is,

$$\sum_{j=1}^2 (-1)^j \int_{S_j} \left[\mathbf{e}_j^{\mathcal{N}}(\mathbf{r}'_j) \cdot \begin{pmatrix} \mathbf{N}_{-mn}^{1,3}(k_1\mathbf{r}'_j) \\ \mathbf{M}_{-mn}^{1,3}(k_1\mathbf{r}'_j) \end{pmatrix} + j\sqrt{\frac{\mu_1}{\epsilon_1}} \mathbf{h}_j^{\mathcal{N}}(\mathbf{r}'_j) \cdot \begin{pmatrix} \mathbf{N}_{-mn}^{1,3}(k_1\mathbf{r}'_j) \\ \mathbf{M}_{-mn}^{1,3}(k_1\mathbf{r}'_j) \end{pmatrix} \right] dS(\mathbf{r}'_j) = 0, \tag{2}$$

for $i = 1, 2, m = -M, \dots, M$ and $n = |m|, \dots, N$. Here, $\mathbf{e}_0, \mathbf{h}_0$ are the tangential components of the incident electric and magnetic field, respectively, and \mathcal{N} is a complex index incorporating M and N . The regular functions

are taken as testing functions in the case $i = 1$, while the radiating functions are taken in the case $i = 2$. In the conventional method the integrals containing the tangential components of the incident field are identified as the expansion coefficients of the external excitation in terms of the regular spherical vector wave functions.

An approximate solution to the scattering problem can be obtained by approximating the surface current densities \mathbf{e}_1 and \mathbf{h}_1 by a linear combination of the tangential components of the regular and radiating single spherical coordinate vector wave functions. For representing the surface current densities \mathbf{e}_2 and \mathbf{h}_2 we use only regular functions. In a compact notation we may write

$$\begin{pmatrix} \mathbf{e}_j^{\mathcal{N}}(\mathbf{r}'_j) \\ \mathbf{h}_j^{\mathcal{N}}(\mathbf{r}'_j) \end{pmatrix} = \sum_{m=-M}^M \sum_{n=|m|}^N a_{mn}^{j\mathcal{N}} \begin{pmatrix} \mathbf{n} \times \mathbf{M}_{mn}^1(k_j \mathbf{r}'_j) \\ -j\sqrt{\frac{\varepsilon_j}{\mu_j}} \mathbf{n} \times \mathbf{N}_{mn}^1(k_j \mathbf{r}'_j) \end{pmatrix} + b_{mn}^{j\mathcal{N}} \begin{pmatrix} \mathbf{n} \times \mathbf{N}_{mn}^1(k_j \mathbf{r}'_j) \\ -j\sqrt{\frac{\varepsilon_j}{\mu_j}} \mathbf{n} \times \mathbf{M}_{mn}^1(k_j \mathbf{r}'_j) \end{pmatrix} \\ + \delta_{j1} \left[c_{mn}^{j\mathcal{N}} \begin{pmatrix} \mathbf{n} \times \mathbf{M}_{mn}^3(k_j \mathbf{r}'_j) \\ -j\sqrt{\frac{\varepsilon_j}{\mu_j}} \mathbf{n} \times \mathbf{N}_{mn}^3(k_j \mathbf{r}'_j) \end{pmatrix} + d_{mn}^{j\mathcal{N}} \begin{pmatrix} \mathbf{n} \times \mathbf{N}_{mn}^3(k_j \mathbf{r}'_j) \\ -j\sqrt{\frac{\varepsilon_j}{\mu_j}} \mathbf{n} \times \mathbf{M}_{mn}^3(k_j \mathbf{r}'_j) \end{pmatrix} \right], \quad (3)$$

where δ_{ji} is the Kronecker symbol.

Once the surface current densities are determined an approximate solution of the scattered field can be obtained by using the Stratton–Chu representation formulas. We note here that our presentation concentrates on the question of obtaining an approximate solution to the scattering problem. In the \mathbf{T} -matrix scheme one additionally expands the scattered field outside a circumscribed sphere of S_1 in terms of spherical vector wave functions, truncates this expansion at the index \mathcal{N} and computes the transition matrix which relates the scattered field coefficients to the incident field coefficients.

The above formalism can be modified by replacing the set of single spherical coordinate vector wave functions $\{\mathbf{M}_{mn}^{1,3}(k\mathbf{r}_i), \mathbf{N}_{mn}^{1,3}(k\mathbf{r}_i)\}_{m \in \mathbb{Z}, n=|m|, \dots}$ by the system of lowest-order spherical vector wave functions $\{\mathbf{M}_{m,|m|+l}^3[k(\mathbf{r}_i - z_p^i \mathbf{e}_3)], \mathbf{N}_{m,|m|+l}^3[k(\mathbf{r}_i - z_p^i \mathbf{e}_3)]\}_{m \in \mathbb{Z}, p=1,2, \dots}$, where $(\mathbf{e}_1, \mathbf{e}_2, \mathbf{e}_3)$ are the unit vectors in Cartesian coordinates, $(z_p^i)_{p=1,2, \dots}$ is a dense sequence of points on a segment of the z -axis and $l = 1$ if $m = 0$ and $l = 0$ otherwise. The sequences of points $(z_p^1)_{p=1,2, \dots}$ and $(z_p^2)_{p=1,2, \dots}$ are located in the interior of S_1 and S_2 , respectively. By employing the same arguments as given by Doicu et al. [4] one can show that the set of integral equations

$$\int_{S_1} \left[[\mathbf{e}_1^{\mathcal{N}}(\mathbf{r}'_1) - \mathbf{e}_0(\mathbf{r}'_1)] \cdot \begin{pmatrix} \mathbf{N}_{-m,|m|+l}^3[k_s(\mathbf{r}'_1 - z_p^1 \mathbf{e}_3)] \\ \mathbf{M}_{-m,|m|+l}^3[k_s(\mathbf{r}'_1 - z_p^1 \mathbf{e}_3)] \end{pmatrix} \right. \\ \left. + j\sqrt{\frac{\mu_s}{\varepsilon_s}} [\mathbf{h}_1^{\mathcal{N}}(\mathbf{r}'_1) - \mathbf{h}_0(\mathbf{r}'_1)] \cdot \begin{pmatrix} \mathbf{N}_{-m,|m|+l}^3[k_s(\mathbf{r}'_1 - z_p^1 \mathbf{e}_3)] \\ \mathbf{M}_{-m,|m|+l}^3[k_s(\mathbf{r}'_1 - z_p^1 \mathbf{e}_3)] \end{pmatrix} \right] dS(\mathbf{r}'_1) = 0, \quad (4)$$

guarantees the null-field condition inside S_1 , and the set of integral equations

$$\sum_{j=1}^2 (-1)^j \int_{S_j} \left[\mathbf{e}_j^{\mathcal{N}}(\mathbf{r}'_j) \cdot \begin{pmatrix} \mathbf{N}_{-m,|m|+l}^{1,3}[k_1(\mathbf{r}'_j - z_p^i \mathbf{e}_3)] \\ \mathbf{M}_{-m,|m|+l}^{1,3}[k_1(\mathbf{r}'_j - z_p^i \mathbf{e}_3)] \end{pmatrix} \right. \\ \left. + j\sqrt{\frac{\mu_1}{\varepsilon_1}} \mathbf{h}_j^{\mathcal{N}}(\mathbf{r}'_j) \cdot \begin{pmatrix} \mathbf{N}_{-m,|m|+l}^{1,3}[k_1(\mathbf{r}'_j - z_p^i \mathbf{e}_3)] \\ \mathbf{M}_{-m,|m|+l}^{1,3}[k_1(\mathbf{r}'_j - z_p^i \mathbf{e}_3)] \end{pmatrix} \right] dS(\mathbf{r}'_j) = 0, \quad (5)$$

with $i = 1, 2$, $m = -M, \dots, M$ and $p = 1, \dots, N$, guarantees the null-field condition outside S_1 and inside S_2 . The surface current densities are now approximated by the complete system of the tangential components of the lowest-order spherical vector wave functions, i.e.

$$\begin{aligned} \begin{pmatrix} \mathbf{e}_j^{\mathcal{N}}(\mathbf{r}'_j) \\ \mathbf{h}_j^{\mathcal{N}}(\mathbf{r}'_j) \end{pmatrix} &= \sum_{m=-M}^M \sum_{p=1}^N a_{mp}^{j\mathcal{N}} \begin{pmatrix} \mathbf{n} \times \mathbf{M}_{m,|m|+l}^1[k_j(\mathbf{r}'_j - z_p^j \mathbf{e}_3)] \\ -j\sqrt{\frac{\varepsilon_j}{\mu_j}} \mathbf{n} \times \mathbf{N}_{m,|m|+l}^1[k_j(\mathbf{r}'_j - z_p^j \mathbf{e}_3)] \end{pmatrix} \\ &+ b_{mp}^{j\mathcal{N}} \begin{pmatrix} \mathbf{n} \times \mathbf{N}_{m,|m|+l}^1[k_j(\mathbf{r}'_j - z_p^j \mathbf{e}_3)] \\ -j\sqrt{\frac{\varepsilon_j}{\mu_j}} \mathbf{n} \times \mathbf{M}_{m,|m|+l}^1[k_j(\mathbf{r}'_j - z_p^j \mathbf{e}_3)] \end{pmatrix} \\ &+ \delta_{j1} \left[c_{mn}^{j\mathcal{N}} \begin{pmatrix} \mathbf{n} \times \mathbf{M}_{m,|m|+l}^3[k_j(\mathbf{r}'_j - z_p^j \mathbf{e}_3)] \\ -j\sqrt{\frac{\varepsilon_j}{\mu_j}} \mathbf{n} \times \mathbf{N}_{m,|m|+l}^3[k_j(\mathbf{r}'_j - z_p^j \mathbf{e}_3)] \end{pmatrix} \right. \\ &\left. + d_{mn}^{j\mathcal{N}} \begin{pmatrix} \mathbf{n} \times \mathbf{N}_{m,|m|+l}^3[k_j(\mathbf{r}'_j - z_p^j \mathbf{e}_3)] \\ -j\sqrt{\frac{\varepsilon_j}{\mu_j}} \mathbf{n} \times \mathbf{M}_{m,|m|+l}^3[k_j(\mathbf{r}'_j - z_p^j \mathbf{e}_3)] \end{pmatrix} \right]. \end{aligned} \quad (6)$$

The total transition matrix for the layered scatterer can be obtained by following the strategy given in a previous paper [5]. Then, the total transition matrix of a multilayered scatterer can be computed by using the recursive scheme elaborated by Peterson and Ström [2].

The advantage of using the system of lowest-order spherical vector wave functions as a system of discrete sources is that for axisymmetric scatterers the problem decouples over the azimuthal modes m . In the case of prolate scatterers, the choice of the multipoles on the axis of symmetry adequately describes the particle geometry. This arrangement is not suitable for oblate scatterers. In this case the procedure of analytic continuation of the representation of the spherical vector-wave functions onto the complex plane along the source coordinate z is used [4]. Essentially, this procedure gives the possibility of correlating the position of the support of discrete sources with the singularities of the analytic continuation of the scattered field inside the layered particle. The spherical vector wave functions can be expressed in terms of the coordinates of the source point $\hat{\mathbf{z}} \in \hat{\Sigma}$ and the observation point $\boldsymbol{\eta} \in \Sigma$ by

$$\mathbf{M}_{mn}^{1,3}(k\mathbf{r}) = z_n^{1,3}(kR) \left\{ jm \frac{P_n^{|m|}(\cos \hat{\theta})}{\sin \hat{\theta}} [\sin(\theta - \hat{\theta}) \mathbf{e}_r + \cos(\theta - \hat{\theta}) \mathbf{e}_\theta] - \frac{dP_n^{|m|}(\cos \hat{\theta})}{d\hat{\theta}} \mathbf{e}_\varphi \right\} e^{jm\varphi} \quad (7)$$

and

$$\begin{aligned} \mathbf{N}_{mn}^{1,3}(k\mathbf{r}) &= \left\{ n(n+1) \frac{z_n^{1,3}(kR)}{kR} P_n^{|m|}(\cos \hat{\theta}) [\cos(\theta - \hat{\theta}) \mathbf{e}_r - \sin(\theta - \hat{\theta}) \mathbf{e}_\theta] \right. \\ &+ \frac{1}{kR} \frac{d}{dR} [Rz_n^{1,3}(kR)] \frac{dP_n^{|m|}(\cos \hat{\theta})}{d\hat{\theta}} [\sin(\theta - \hat{\theta}) \mathbf{e}_r + \cos(\theta - \hat{\theta}) \mathbf{e}_\theta] \\ &\left. + jm \frac{1}{kR} \frac{d}{dR} [Rz_n^{1,3}(kR)] \frac{P_n^{|m|}(\cos \hat{\theta})}{\sin \hat{\theta}} \mathbf{e}_\varphi \right\} e^{jm\varphi}, \end{aligned} \quad (8)$$

where $z_n^{1,3}(kR)$ denotes the spherical Bessel functions or the spherical Hankel functions, respectively, $(\mathbf{e}_r, \mathbf{e}_\theta, \mathbf{e}_\varphi)$ are the unit vectors in spherical coordinates, $P_n^{|m|}$ are the Legendre functions and

$$R^2 = \rho^2 + (z - \hat{\mathbf{z}})^2, \quad \sin \hat{\theta} = \frac{\rho}{R}, \quad \cos \hat{\theta} = \frac{z - \hat{\mathbf{z}}}{R}.$$

The complex plane $\widehat{\Sigma} = \{\widehat{\mathbf{z}} = (\text{Re } \widehat{\mathbf{z}}, \text{Im } \widehat{\mathbf{z}}) / \text{Re } \widehat{\mathbf{z}}, \text{Im } \widehat{\mathbf{z}} \in \mathbf{R}\}$ is defined such that real axis $\text{Re } \widehat{\mathbf{z}}$ coincides with the z -axis of the azimuthal plane $\varphi = \text{const}$, $\Sigma = \{\boldsymbol{\eta} = (\rho, z) / \rho \geq 0, z \in \mathbf{R}\}$. The region in which the spherical vector wave functions are analytical with respect to the variable $\widehat{\mathbf{z}}$ is the domain \widehat{D} whose boundary coincides with the image of the generator of revolution. Note that a point $\widehat{\mathbf{z}} \in \widehat{\Sigma}$ is called the image of a point $\boldsymbol{\eta} \in \Sigma$ if $R_{\boldsymbol{\eta}\widehat{\mathbf{z}}}^2 = 0$. In this case, for a sequence of poles distributed symmetrically with respect to the $\text{Re } \widehat{\mathbf{z}}$ -axis and having at least two limit points in \widehat{D} , we can construct an approximate solution by using (4), (5) and (6).

3. Numerical results

The formulation presented in Section 2 has been implemented in a computer program. In this section we present computer results for prolate and oblate layered spheroids. The scatterer coordinate system is denoted by $Oxyz$ with the z -axis directed along the symmetry axis of the scatterer. For simplicity we assume that the incident wave is a plane wave traveling along the symmetry axis of the scatterer. The polarization direction encloses an angle α_{pol} with the x -axis. The layered scatterer consists of two spheroids with a common axis of symmetry. The semi-axes of the external spheroid are denoted by a_1 and b_1 , while the semi-axes of the internal spheroid are denoted by a_2 and b_2 . The refractive indices are $m_1 = 1.5$ and $m_2 = 1.8$, respectively. The internal spheroid can be shifted along the axis of symmetry with a distance z_2 . Specifically, the differential scattering cross section (DSCS) normalized by πa_1^2 will be computed for parallel and perpendicular polarization of the incident wave.

In our first example we consider a prolate layered scatterer with $k_s a_1 = 6$, $k_s b_1 = 3$ and $k_s a_2 = 3$, $k_s b_2 = 1.5$. We choose $k_s z_2 = 0$ and $k_s z_2 = 0.5$. The results corresponding to the null-field method with localized and distributed sources are shown in Fig. 2. For this case we used a collection of multipoles located on the symmetry axis of the scatterer. The complete agreement between the curves serves as an evidence for the accuracy of the proposed method. In Fig. 3 we plot the differential scattering cross section for a layered scatterer with $k_s a_1 = 10$, $k_s b_1 = 1$ and $k_s a_2 = 4$, $k_s b_2 = 0.5$. Only the results corresponding to the null-field method with distributed sources are shown since the null-field method with localized sources fails to converge.

The next problem is that of an oblate layered spheroid with $k_s a_1 = 3$, $k_s b_1 = 5$ and $k_s a_2 = 1$, $k_s b_2 = 2$. The results plotted in Fig. 4 clearly demonstrate that no significant differences exist between the scattering diagrams. For this type of scatterer we choose the multipoles on the imaginary axis in the complex plane. The positions of the

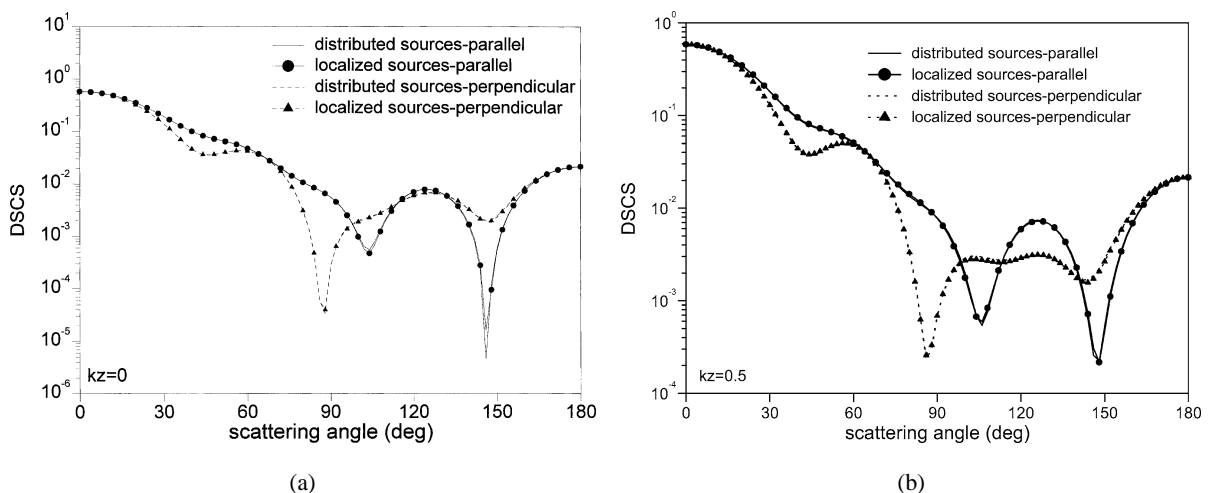


Fig. 2. Differential scattering cross section for a layered prolate scatterer with $k_s a_1 = 6$, $k_s b_1 = 3$, $m_1 = 1.5$ and $k_s a_2 = 3$, $k_s b_2 = 1.5$, $m_2 = 1.8$. The results are computed with the null-field method with localized and distributed sources for: (a) $k_s z_2 = 0$ and (b) $k_s z_2 = 0.5$.

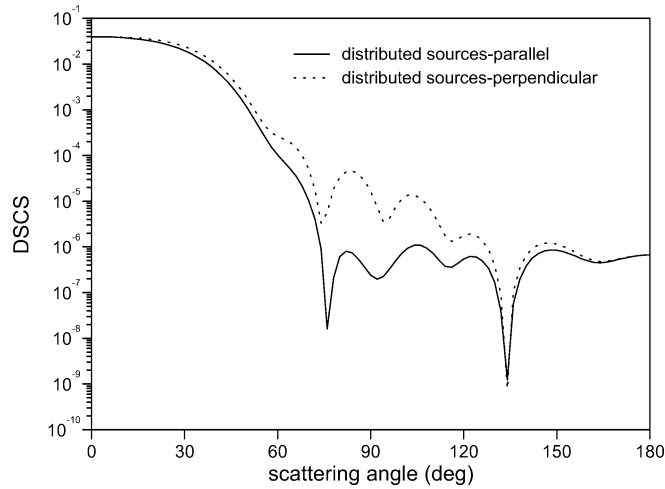


Fig. 3. Differential scattering cross section for a layered prolate scatterer with $k_s a_1 = 10$, $k_s b_1 = 1$, $m_1 = 1.5$ and $k_s a_2 = 4$, $k_s b_2 = 0.5$, $m_2 = 1.8$. The results are computed with the null-field method with distributed sources for $k_s z_2 = 0$.

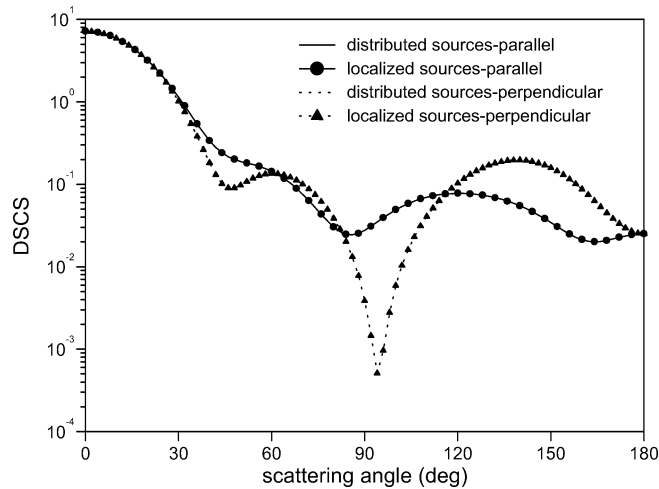


Fig. 4. Differential scattering cross section for a layered oblate scatterer with $k_s a_1 = 3$, $k_s b_1 = 5$, $m_1 = 1.5$ and $k_s a_2 = 1$, $k_s b_2 = 2$, $m_2 = 1.8$. The results are computed with the null-field method with localized and distributed sources for $k_s z_2 = 0$.

distributed sources are shown in Fig. 5. Plots of the differential scattering cross section for an oblate spheroid with $k_s a_1 = 1$, $k_s b_1 = 5$ and $k_s a_2 = 0.5$, $k_s b_2 = 2$ are shown in Fig. 6. As before, the null-field method with localized sources does not converge for this geometry.

4. Conclusions

A novel formulation of the null-field method with distributed sources for layered scatterers has been proposed. In this method we choose the tangential components of the lowest-order multipoles with different origins as a complete system of functions on the particle surface. The advantage of the proposed approach over the conventional

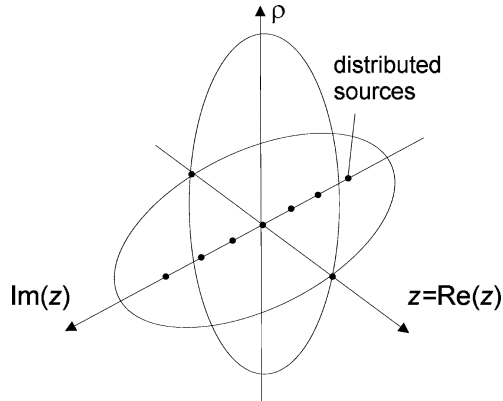


Fig. 5. Position of distributed sources in the complex plane.

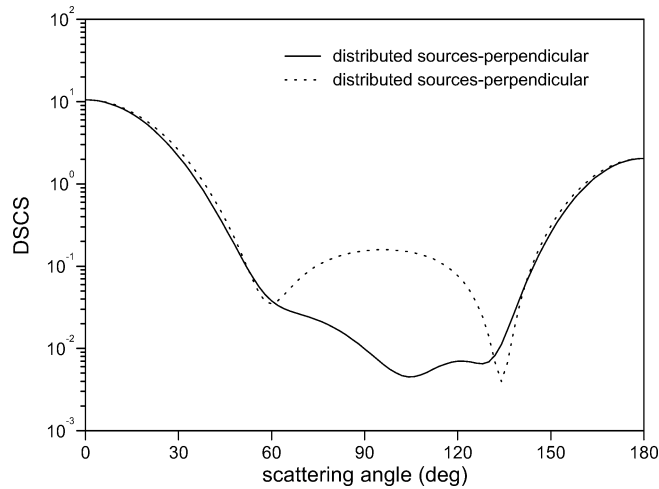


Fig. 6. Differential scattering cross section for a composite oblate scatterer with $k_s a_1 = 1$, $k_s b_1 = 5$, $m_1 = 1.5$ and $k_s a_2 = 0.5$, $k_s b_2 = 2$, $m_2 = 1.8$. The results are computed with the null-field method with distributed sources for $k_s z_2 = 0$.

method concerning the applicability to highly elongated and flattened scatterers have been demonstrated for a number of examples.

References

- [1] D.S. Wang, P.W. Barber, Scattering by inhomogeneous nonspherical objects, *Appl. Opt.* 18 (1979) 1190–1197.
- [2] B. Peterson, S. Ström, T-matrix formulation of electromagnetic scattering from multilayered scatterers, *Phys. Rev. D* 10 (1974) 2670–2684.
- [3] A. Doicu, T. Wriedt, Extended boundary condition method with multipole sources located in the complex plane, *Optics Commun.* 139 (1997) 85–91.
- [4] A. Doicu, Y. Eremin, T. Wriedt, *Acoustic and Electromagnetic Scattering Analysis using Discrete Sources*, Academic Press, London, 2000.
- [5] A. Doicu, T. Wriedt, Calculation of the T-matrix in the null-field method with discrete sources, *J. Opt. Soc. Amer. A* 16 (1999) 2539–2544.